Density fluctuations in liquid rubidium. I. Neutron-scattering measurements*

J. R. D. Copley†
Solid State Science Division, Argonne National Laboratory, Argonne, Illinois 60439

J. M. Rowe
Solid State Science Division, Argonne National Laboratory, Argonne, Illinois 60439
and Institute for Materials Research, National Bureau of Standards, Washington, D. C. 20234

(Received 15 November 1973)

We report neutron-scattering measurements of the coherent scattering function $S(Q,\omega)$ of liquid rubidium at 315 K, in the range of wave vectors $1.25 \leq Q \leq 5.5$ Å^{-1}. In this range there is no evidence of peaks at finite ω in $S(Q,\omega)$ plotted at constant Q. On the other hand the Fourier transform $F(Q,t)$ exhibits structure, notably for $Q = 2.0$ Å^{-1}, which indicates at least two characteristic (wavelength-dependent) relaxation times in the liquid. For wave vectors >3.0 Å^{-1}, $F(Q,t)$ may be characterized by a single relaxation time. These results, in conjunction with our results for $Q < 1.0$ Å^{-1}, offer the possibility of detailed comparisons with models of the liquid state and with molecular-dynamics calculations.

I. INTRODUCTION

In this paper we report comprehensive measurements of the coherent scattering function of liquid rubidium at 315 K, using the inelastic neutron-scattering technique. The results have been corrected for all known experimental factors, using data-analysis[1] and multiple-scattering[2] programs which were developed at this laboratory. In a recent paper[3] the coherent and incoherent scattering functions of liquid argon were presented, and in a forthcoming paper[4] we shall describe neutron scattering measurements on molten rubidium bromide. It is our intent to make systematic measurements on a series of typical simple liquids, in an attempt to clarify the physics underlying the dynamics of these systems.

Rubidium was chosen for this study for two reasons. First, the dispersion relations for solid Rb have been measured in some detail,[5] and used to derive a volume-dependent "effective two-body potential,"[6] which gives good agreement with the equilibrium properties of liquid Rb. Second, the neutron scattering cross section[7,8] is almost totally coherent, so that the coherent-scattering function can be measured separately (in contrast with other alkali metals,[9] where the incoherent cross section is of the same order of magnitude as the coherent cross section). In this regard it should be noted that by using different isotopic mixtures of ^{6}Li and ^{7}Li, both the coherent and incoherent scattering functions might be obtained, as was done for argon. However, the large absorption cross section of ^{6}Li (945 b) makes this experiment very difficult, and the fact that ^{6}Li and ^{7}Li both have large incoherent cross sections would preclude extending the measurements of the coherent scattering function to small momentum transfers.

In many theoretical models[10,11] of the liquid state, the scattering function is expressed in terms of its low-order energy moments, sometimes including an adjustable parameter. The usefulness of neutron scattering experiments on liquids has been questioned[12] on the basis of the qualitative agreement with the results obtained from these models, implying that the low order moments characterize the function. However, experiments have shown that the fourth energy moment is required to obtain agreement, and this moment depends explicitly on the interatomic potential. After all, the fourth energy moment of the scattering function *completely* characterizes a purely harmonic solid, the normalized fourth moment being nothing more than the "dynamical matrix." Thus the systematic testing of theories of liquids which correctly incorporate moments up to the fourth or higher, serves both to probe the interatomic potential (predominantly at short distances which are not sampled by atoms in solids), and to test the approximations inherent in the theories. Furthermore, detailed comparisons between experimental results and the results of "molecular-dynamics" calculations can test both the validity of the molecular-dynamics approach to particular systems and the assumed potential. In the following paper[13] such a comparison is carried out for the case of liquid rubidium. Good agreement with the present results is obtained, using the effective two-body potential of Ref. 6.

The present measurements cover the range of wave vectors Q from 1.25 to 5.5 Å^{-1}. In Sec. II we describe the experimental measurements and

the data reduction. The results are presented in Sec. III. They include some of the results of a separate experiment, in the range $0.3 \leq Q \leq 1.0$ Å^{-1}, which is reported elsewhere.[14] Section IV contains the conclusions we have drawn from this work.

II. MEASUREMENTS AND DATA REDUCTION

In an inelastic-neutron-scattering experiment, one seeks to measure the double differential cross section

$$\frac{d^2\sigma}{d\Omega\, d\omega}(\vec{k}_0 \to \vec{k}) = \frac{\sigma_B}{4\pi}\,\frac{k}{k_0}\,S(\vec{Q},\omega),$$

for single scattering from incident wave vector $\vec{k}_0$ to scattered wave vector $\vec{k}$. Here $d\Omega$ is the solid angle, σ_B is the bound-atom scattering cross section, $\hbar\vec{Q} = \hbar(\vec{k}_0 - \vec{k})$ is the momentum transferred to the system, and $\hbar\omega = (\hbar^2/2m_n)(k_0^2 - k^2)$ is the energy transferred to the system: m_n is the mass of the neutron, and $S(\vec{Q},\omega)$ is the scattering function of Van Hove.[15] It is the quantity of most interest since it is only related to the properties of the system under study. In the case of an isotropic system, only the magnitude of $\vec{Q}$ is relevant, so one is concerned with the isotropic function $S(Q,\omega)$. The symmetrized scattering function is defined by

$$\tilde{S}(Q,\omega) = e^{-\hbar\omega/2k_BT}S(Q,\omega),$$

where k_B is Boltzmann's constant and T is the temperature of the system.

The measurements were made using the hybrid time-of-flight spectrometer[16] at the Argonne CP-5 reactor. Measurements were made with two different incident neutron energies E_0, 4.94 and 33.0 meV, with over-all energy resolutions [full width at half-maximum (FWHM)] of 0.24 and 1.0–1.15 meV, respectively. We shall refer to these two sets of measurements as experiments 1 and 2.

For experiment 1, using the lower incident energy, measurements were made at 31 scattering angles φ ranging from 17.4° to 118.8° (elastic Q's, defined by $Q = 2k_0 \sin\frac{1}{2}\varphi$, ranging from 0.5 to 2.7 Å^{-1}). Single detectors were used in the vicinity of the first peak in the structure factor $Q_0 \simeq 1.53$ Å^{-1}, giving a resolution in Q (FWHM) of 0.01 Å^{-1}: at the lower and higher angles, two or three detectors were ganged together, resulting in resolutions of ~0.025 Å^{-1}. Data at the highest angle were marred by the (111) aluminum Bragg peak from the sample container. For the second experiment, using the higher incident energy, measurements were made at 15 angles from 26.4° to 108.0° (elastic Q's from 1.8 to 6.5 Å^{-1}). The scattering angles were chosen to avoid picking up Bragg peaks from the container. The resolution in Q was ~0.05 Å^{-1}.

The rubidium, obtained commercially (quoted purity 99.9%), was contained in a cylindrical aluminum container, o.d. 1.68 cm, wall thickness 0.045 cm, with a usable sample height of 9.6 cm. Horizontal disks made of boron nitride (0.09 cm thick), separated by 1.68 cm, were used to reduce multiple-scattering effects.[17] The sample container had heaters at top and bottom, and was surrounded by several layers of aluminum foil used as radiation shields. The temperature was controlled at 315 K to within ±3 K, and the temperature difference across the sample was generally less than 1 K.

Separate runs were made with the rubidium in the container and with the empty container. For the higher-energy experiment, time-independent backgrounds were measured by placing a cadmium shutter[16] in the beam for 1 min in every 30 min. This shutter was not available at the time of experiment 1. Experimental runs were also made[1] in order to normalize the data, to determine the timing of the incident beam, and to measure the energy resolution. The latter measurements were made using an aluminum container, identical to the container used for the sample measurements, but filled with ~0.5 g cotton: the widths of the incoherent elastic peaks due to the hydrogen scattering were determined.

Representative plots of the raw data are shown in Fig. 1 for both incident energies. The container run has been normalized to the sample run. The energy resolution is indicated by the width of the elastic peak from the aluminum container. In Fig. 2 the same data are shown after conversion to the form of a symmetrized scattering function $\tilde{S}(Q,\omega)$. Time-independent backgrounds were first subtracted from the raw data, and the container counts were then corrected for attenuation in the presence of the sample (this correction factor is between 0.93 and 0.94 in all cases). The data shown in Fig. 2 have been corrected for self-shielding, but not for multiple scattering. The self-shielding factor, calculated following Carpenter,[18] is between 0.91 and 0.92. Shielding by the container represents a further 0.9% correction. Multiple scattering contributions, and the total cross section of rubidium, were calculated using the program MSCAT.[2] These contributions are shown in Fig. 2. Note that in most cases the multiple scattering is multiplied by a factor of 10. The multiple scattering was calculated using the kernel $\tilde{S}(Q,\omega)$ obtained by Rahman[13]; beyond $Q \sim 3.6$ Å^{-1}, the model kernel of Pathak and Singwi[19] was used. Multiple-scattering contributions were also computed using the Pathak-Singwi kernel exclusively. The zeroth and fourth classical energy moments, which constitute the input to this model for the kernel, were obtained from the effective potential of

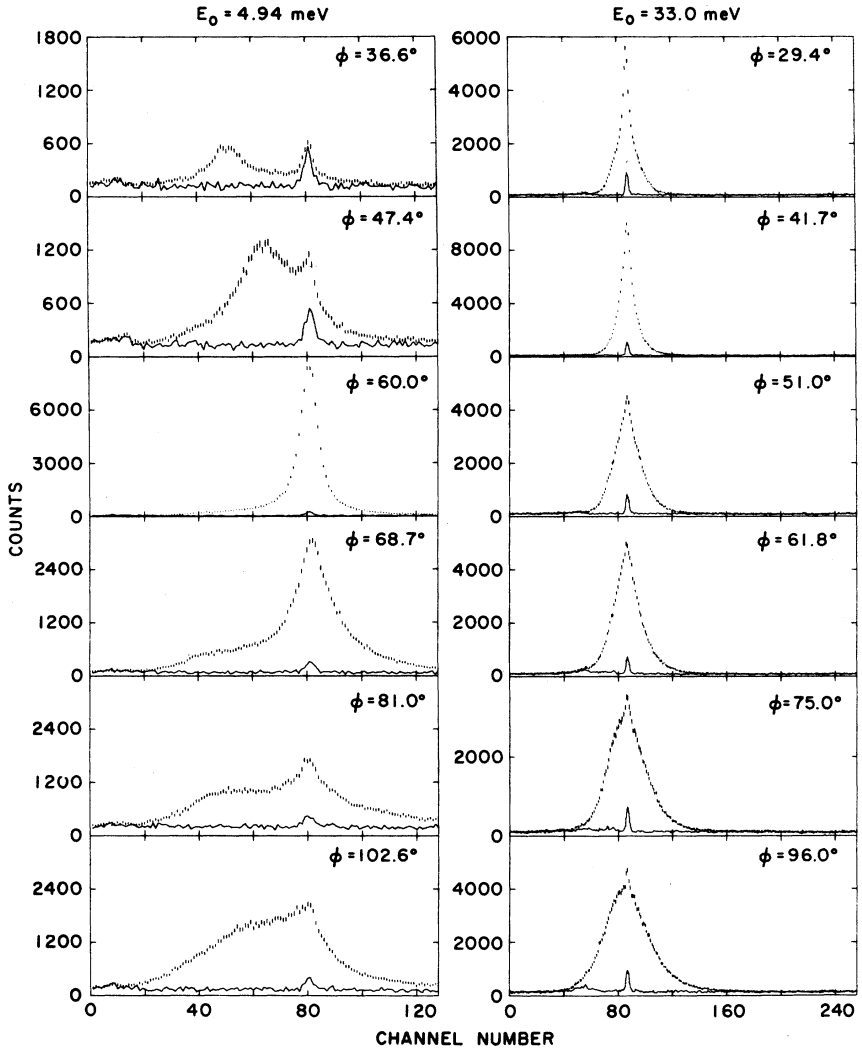

FIG. 1. Plots of raw data from the two experiments. The horizontal axis is proportional to neutron time of flight. The normalized counts from the empty container are indicated by continuous lines.

Ref. 6 and a pair-distribution function obtained from the molecular-dynamics calculations.[13] The sensitivity of the moments to the kernel used in the multiple scattering correction is discussed in Sec. III.

It is instructive to examine the data shown in Figs. 1 and 2 for $E_0 = 4.94$ meV and $\varphi = 36.6°$. The "inelastic" peak in the raw data is largely due to the well-known t^4 factor which must be included in order to obtain $S(Q, \omega)$. A similar peak is evident in the plot for $\varphi = 47.4°$ in Fig. 1. Note that the peak at $\varphi = 36.6°$ persists when the data are plotted on an energy scale (Fig. 2). Since the wave vector Q is changing with ω, an apparent inelastic peak may show up in a constant-angle plot, depending on the detailed topology of $S(Q, \omega)$, even when there are no inelastic peaks in plots of $S(Q, \omega)$ at constant Q. This occurs most frequently when Q is somewhat smaller than Q_0, and E_0 is small. In the past, peaks such as those shown in Figs. 1 and 2 have been used to produce a dispersion curve for the liquid. We emphasize that in the range $1.25 \leq Q \leq 5.5$ Å^{-1}, no inelastic peaks exist in plots of $\tilde{S}(Q, \omega)$ at constant Q. On the other hand such peaks *do* exist at smaller values of Q.[14]

III. ANALYSIS OF RESULTS

Having subtracted the multiple scattering, the data at different angles were interpolated to selected values of Q, and then corrected for energy resolution. Representative plots of $\tilde{S}(Q, \omega)$, at four values of ω, are shown in Fig. 3. The data from the two experiments are indicated by different symbols. Note the change of scale, in the plot for $\omega = 0.0$ ps^{-1}, in the region of $Q \sim Q_0$. It is immediately apparent that the data from the two experiments do not join smoothly for $\omega = 0.0$ ps^{-1}, whereas at $\omega = 2.0$ ps^{-1} the agreement is much improved. The lack of agreement at very small ω is believed to

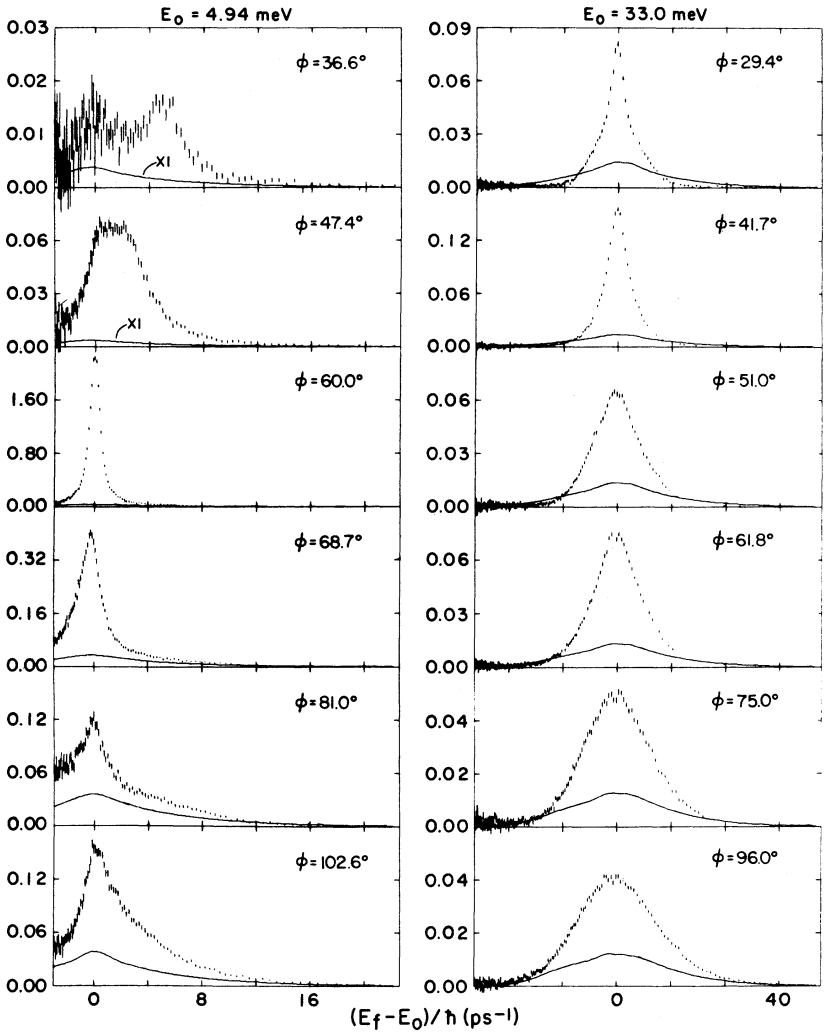

FIG. 2. Plots of the scattering function $\tilde{S}(Q,\omega)$ at constant angle, from the two experiments. The computed multiple scattering is indicated by the continuous curve. In every case, except for the two lowest angles in the 4.94-meV experiment, the multiple scattering has been multiplied by a factor of 10.

be a resolution effect. The results from experiment 1 are clearly superior, because of the better energy resolution. These results indicate structure in $\tilde{S}(Q,\omega)$, for Q's between ~2 and ~3 Å^{-1}, comprising a narrow peak superimposed upon a broad peak. Because of the poorer energy resolution of experiment 2, this peak cannot be correctly unfolded by the resolution correction program. As a result $\tilde{S}(Q,\omega)$ is depressed for small ω, and the FWHM of $\tilde{S}(Q,\omega)$ is too large. The over-all agreement between the two experiments, for larger values of ω, is very satisfactory.

In Figs. 4–6 we show a series of constant Q plots of $\tilde{S}(Q,\omega)$. The plots for $1.25 \leq Q \leq 2.5$ Å^{-1} (Fig. 5) and for $3.0 \leq Q \leq 5.5$ Å^{-1} (Fig. 6) were obtained from experiments 1 and 2, respectively. We also show (Fig. 4) three plots for $Q \leq 1$ Å^{-1}, obtained from a separate experiment.[14] The results of experiment 1 can be used to construct $\tilde{S}(Q,\omega)$ for $Q=1.0$ Å^{-1}, although the statistical accuracy is low. In fact, this result was used to help establish the normalization of the small-Q experiment, as discussed in detail in Ref. 14. A smoothed representation of the $\tilde{S}(Q,\omega)$ obtained from experiment 1 is shown as the solid line for $Q=1.0$ Å^{-1} in Fig. 4. The points shown in Figs. 5 and 6 were obtained from a sum of Gaussian functions, as described in Ref. 1. To the extent that a functional form was fitted to the data, the points in Figs. 5 and 6 are smoothed. The errors were estimated from the errors in the raw data, and from the size and reliability of the resolution correction. The data from experiment 1 are unaffected by this correction, except at $Q=1.5$ Å^{-1}. Furthermore, the data from experiment 2 are considered reliable, except at $Q=3.0$ Å^{-1}, where there is still some evidence of a narrow peak superimposed upon a broader peak.

In Fig. 5 we see discontinuities in the slope of $\tilde{S}(Q,\omega)$, in particular for $Q=2.0$ and 2.25 Å^{-1}. Although the exact shape of the results may be sen-

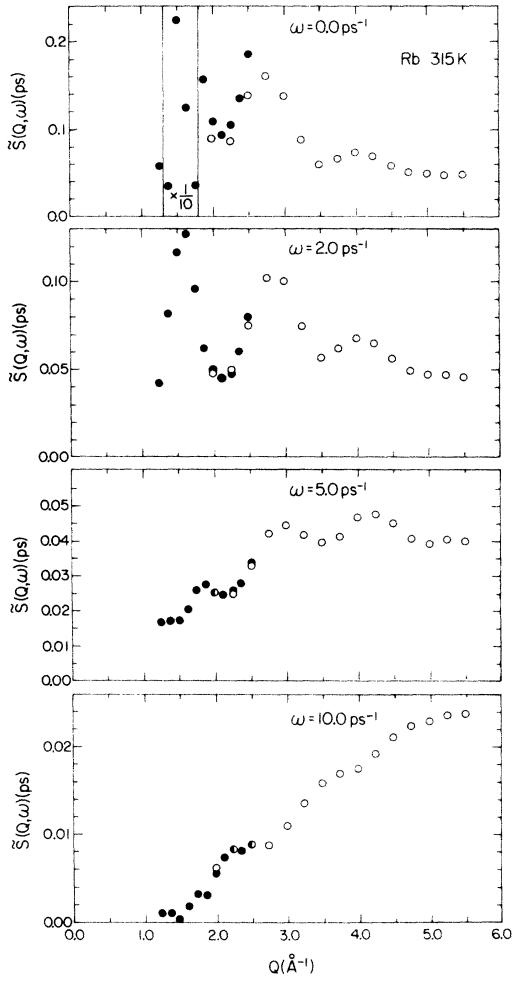

FIG. 3. Corrected scattering function $\tilde{S}(Q,\omega)$ for four values of ω. Note the change of scale in the top plot, in the region of the principal peak in the structure factor. The closed and open circles refer to experiments 1 and 2, respectively.

sitive to the method of correction for energy resolution, there is no doubt that such features do exist in the data. The molecular-dynamics calculations[13] also show such effects, which are related to the existence of two distinct relaxation processes in this region of momentum transfers.

In order to test the over-all validity of the data, we have calculated the zeroth and first energy moments of $S(Q,\omega)$. The zeroth moment

$$\int_{-\infty}^{\infty} S(Q,\omega)\,d\omega = S(Q)$$

is shown in Fig. 7 together with the molecular-dynamics results,[13] and the neutron diffraction results of Page *et al.*[20] The present data oscillate about a value of about 1.04 at the larger Q's. There appears to be an over-all error in the normalization of our data, which is probably due to poor performance of the beam monitors. Apart from this discrepancy, the data are in good agreement with Rahman's calculations[13] except at $Q \simeq Q_0$. In this region there is considerable experimental data, and we believe the present results are good to better than 5%. On the other hand there are sizable discrepancies between our data and those of Page *et al.*,[20] especially in the region $1.25 < Q < 1.5$ Å^{-1}. At larger values of Q, the oscillations in $S(Q)$ obtained from this experiment and from the molecular dynamics calculation are not in phase with those of Ref. 20.

The first moment, divided by the exact theoretical value,[21]

$$\langle\omega\rangle_{\text{exact}} \equiv \int_{-\infty}^{\infty} \omega S(Q,\omega)\,d\omega = \frac{\hbar Q^2}{2M},$$

where M is the mass of a rubidium atom, is shown in Fig. 8. Here the moments are on average ~11% high. This increased discrepancy might indicate an inadequate correction for multiple scattering. However, our own calculations indicate that this correction is -0.04 ± 0.004 for $S(Q)$, and between 10 and 30%, with a possible error of ±2% in the case of $\langle\omega\rangle$. The errors were obtained from a comparison between calculations using two different choices of kernel (Sec. II). In the region of Q's between 2.0 and 2.75 Å^{-1}, in the case of experiment 2, the high values of $\langle\omega\rangle$ are probably due to the inadequate correction for energy resolution described above. At larger values of Q, the fluctua-

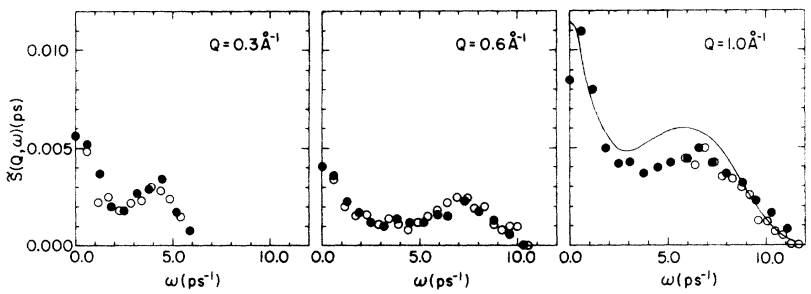

FIG. 4. Scattering function $\tilde{S}(Q,\omega)$ for three values of $Q \simeq 1.0$ Å^{-1}. These results were obtained from a separate experiment (Ref. 14). The solid line in the $Q = 1.0$-Å^{-1} plot is a smoothed representation of the $\tilde{S}(Q,\omega)$ derived from experiment 1. (See text.) Closed circles: energy-gain data; open circles: energy-loss data.

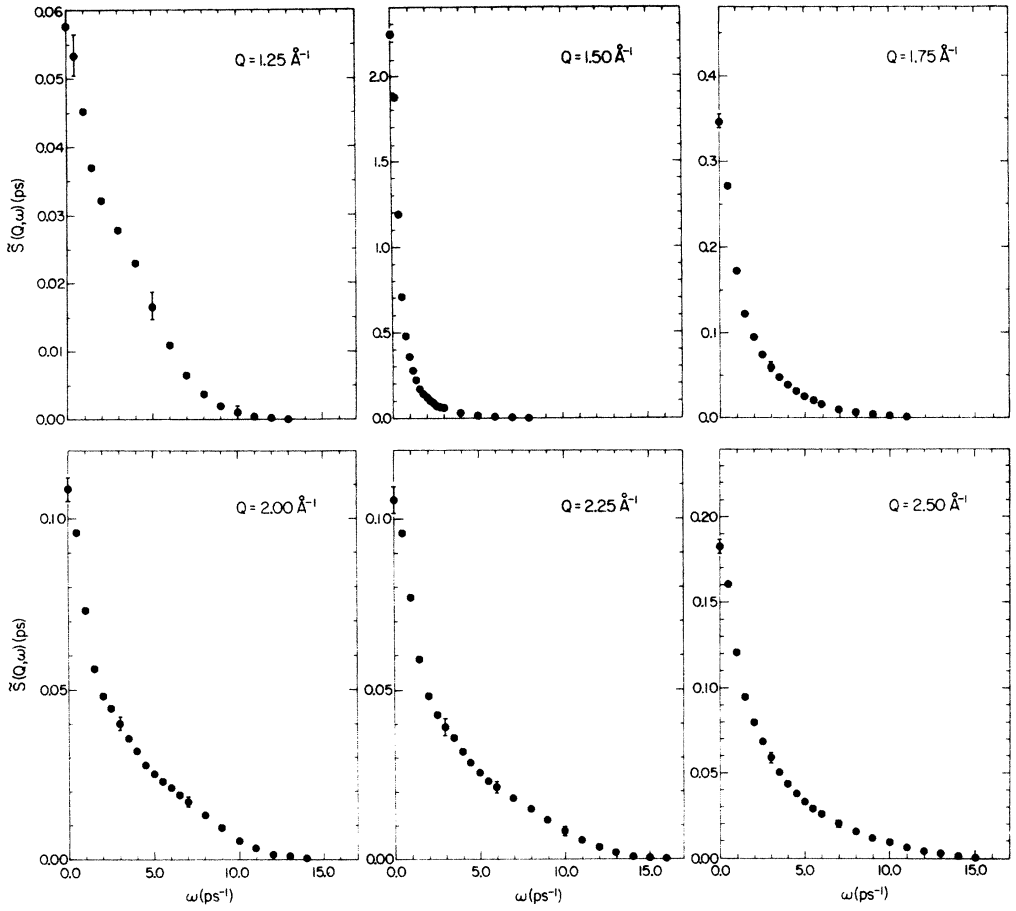

FIG. 5. Scattering function $\tilde{S}(Q,\omega)$ for six values of Q between 1.25 and 2.5 Å^{-1}. These results were obtained from experiment 1.

tions in $\langle\omega\rangle$ are probably related to the relatively large statistical errors in the large-energy-transfer regions of $\tilde{S}(Q, \omega)$.

The agreement between the results obtained from this experiment and the independent values of $S(Q)$ and $\langle\omega\rangle$ is a good indication of the over-all reliability of the data presented here. We would reemphasize the absolute necessity for such comparisons in assessing the reliability of experimental data on $S(Q, \omega)$. As the data presented here were absolutely normalized with *no* adjustable parameters, reasonable agreement for the zeroth and first energy moments is a necessary but not sufficient test for the reliability of the data. It should also be noted that, as discussed in Ref. 3, the first moment is a very stringent test of the high-energy-transfer region of $S(Q, \omega)$ where both the statistical errors and the multiple-scattering corrections are largest.

In Figs. 9 and 10 we show plots of the intermediate-scattering function

$$F(Q, t)=\int_{-\infty}^{\infty} S(Q, \omega)e^{i\omega t}\, d\omega\,,$$

which was obtained from the $\tilde{S}(Q, \omega)$ plots shown in Figs. 5 and 6. Since the final $\tilde{S}(Q, \omega)$ is written as a sum of Gaussians, the Fourier transforms are easily obtained.[22] The plots of $F(Q, t)$ for $Q \leq 2.5$ Å^{-1}, are of particular interest. Except at $Q = 1.5$ and 1.75 Å^{-1}, there is clear evidence of structure which indicates at least two characteristic relaxation times. This structure is also observed in the molecular dynamics calculations.[13] An attempt to fit $F(Q, t)$ at $Q = 2.0$ Å^{-1} using a Gaussian memory function with a single relaxation time proved unsuccessful. On the other hand, the same approach works well over the entire region of measured momentum transfers in the case of liquid argon.[23] The $F(Q, t)$ obtained from this experiment is compared with molecular dynamics results in the following paper.[13]

In Fig. 11 we show the full width at half-maximum height of $\tilde{S}(Q, \omega)$. Again we note the lack of

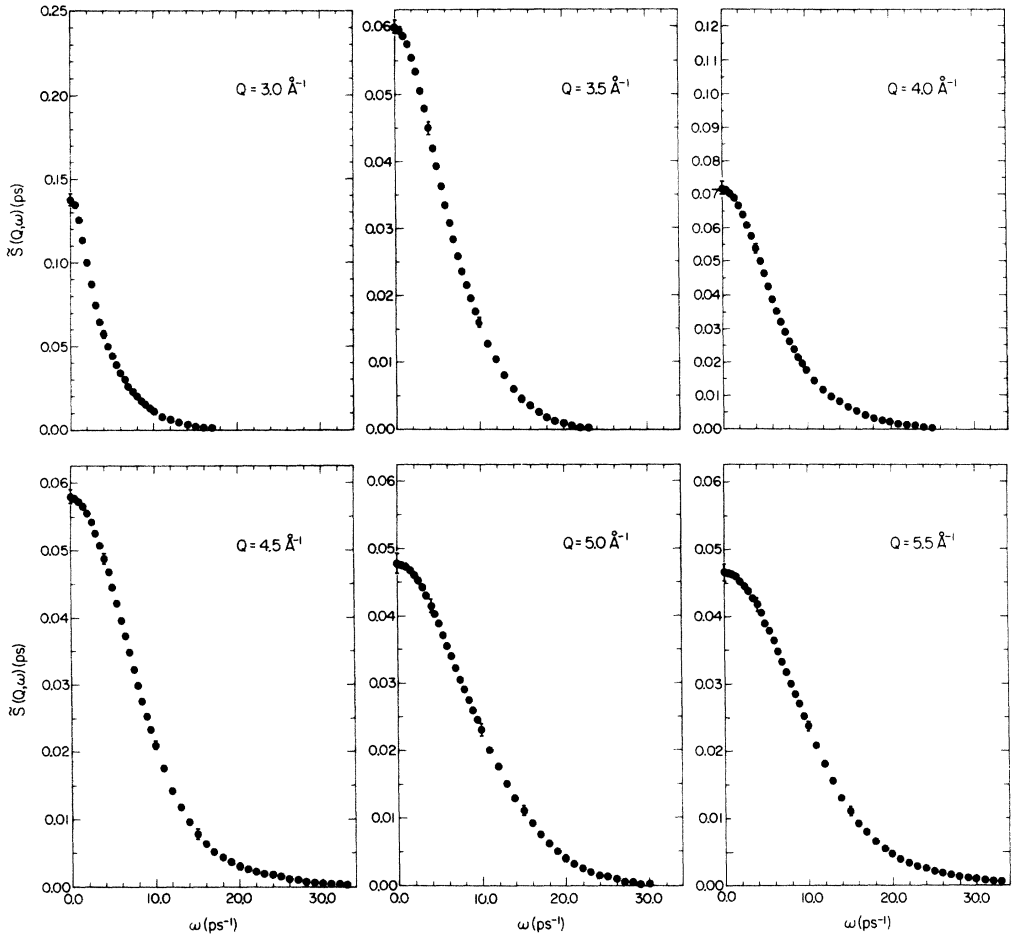

FIG. 6. Scattering function $\tilde{S}(Q,\omega)$ for six values of $Q \geq 3.0$ Å^{-1}. These results were obtained from experiment 2.

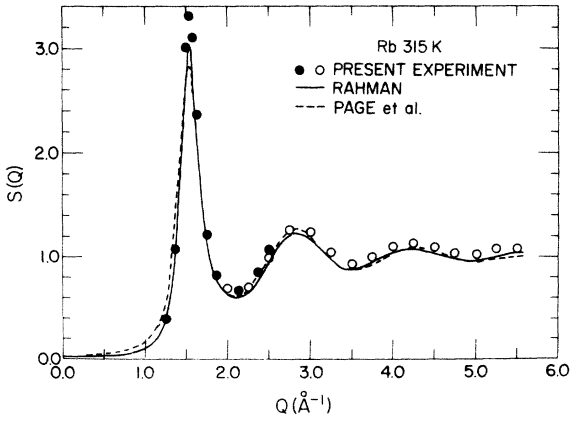

FIG. 7. Structure factor $S(Q)$, as obtained from the present experiment, from the molecular-dynamics results (Ref. 13) and from the work of Page *et al.* (Ref. 20). The symbols have the same significance as in Fig. 3.

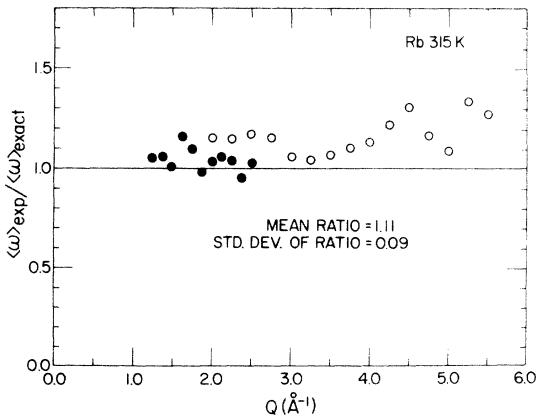

FIG. 8. Ratio of the experimental first moment to the theoretical result. The symbols have the same significance as in Fig. 3.

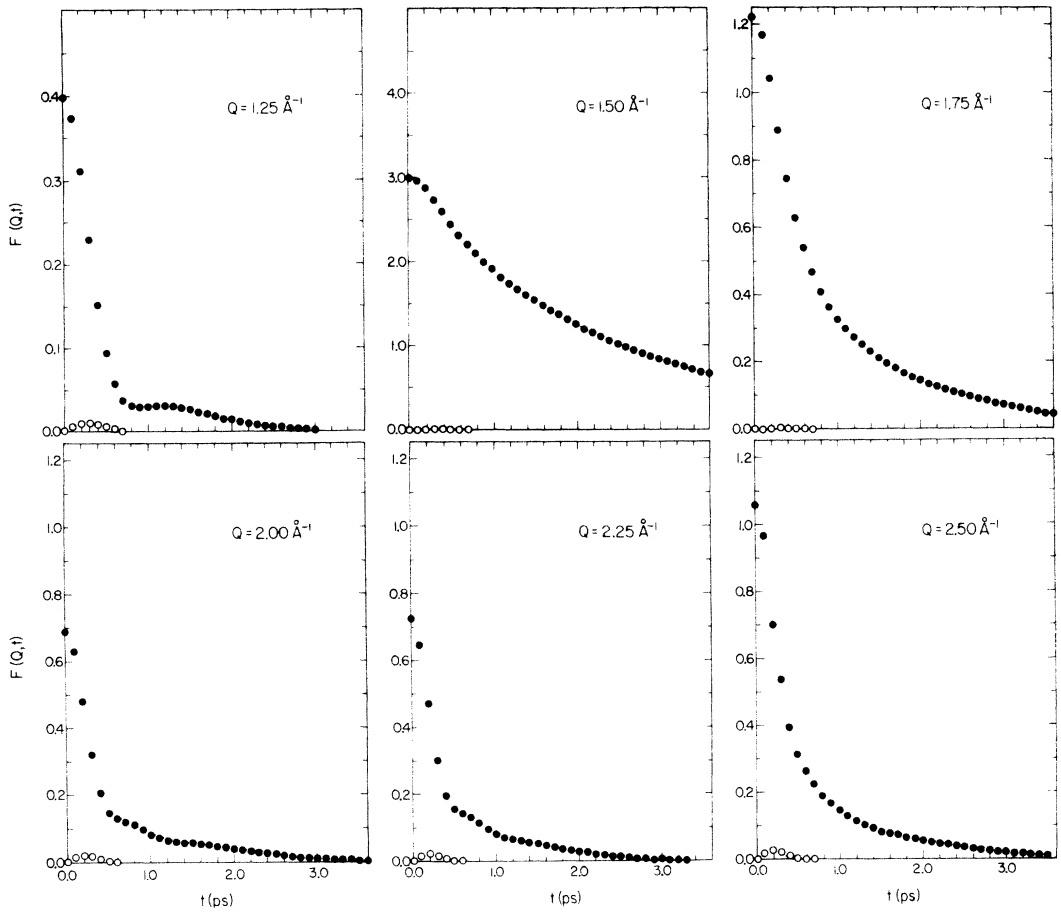

FIG. 9. Intermediate-scattering function $F(Q,t)$ for six values of Q between 1.25 and 2.5 Å^{-1}. The real and imaginary parts are represented by closed and open circles, respectively.

agreement between the two experiments. Since the narrow peak in $\tilde{S}(Q,\omega)$ is not properly extracted in experiment 2, the FWHM is artificially augmented. At larger values of Q, the widths approach the ideal-gas limit

$$\Delta_{\text{FWHM}}(\text{i,g}) = 2[2(\ln 2)kT/M]^{1/2}Q\ .$$

In the vicinity of $Q = Q_0$ our results compare very well with those of Suck and Gläser.[24] We are however in definite disagreement in the region of the second peak. Though the lower-resolution results (the open circles) are no doubt too high, particularly at $Q \leq 2.5$ Å^{-1}, resolution effects are becoming less important at $Q = 3.0$ Å^{-1} and here the two sets of data differ by a factor of 2. The reason for this is unknown. The calculations of Rahman[13] support the present measurements. The measurements of Egelstaff *et al.*[25] on Rb at 200°C only extend down to $Q \sim 4$ Å^{-1}, so no conclusions concerning the widths for $Q \approx 2.8$ Å^{-1} can be drawn from their work.

We also show in Fig. 11 the mean frequency ω_m, which was obtained as the average of the two frequencies corresponding to the half-height of $S(Q,\omega)$. The ideal gas value is simply given by

$$(\omega_m)_{\text{i.g.}} = \hbar Q^2/2M\ .$$

Both ω_m and the FWHM show oscillatory behavior. Such behavior has been observed in both helium[26] and neon.[27] As was pointed out by Buyers *et al.*,[27] this behavior reflects oscillations in the higher moments of $S(Q,\omega)$, which do not decay as rapidly as the oscillations in $S(Q)$. In general, this type of behavior is to be expected in all liquids.[28]

IV. DISCUSSION

In Sec. III we have described the results of measurements of the coherent scattering function of liquid rubidium for wave vectors between 1.25 and 5.5 Å^{-1}. In an earlier paper,[14] similar results were presented for wave vectors between 0.3 and 1.0 Å^{-1}. These two experiments provide a detailed description of the dynamical properties of this sim-

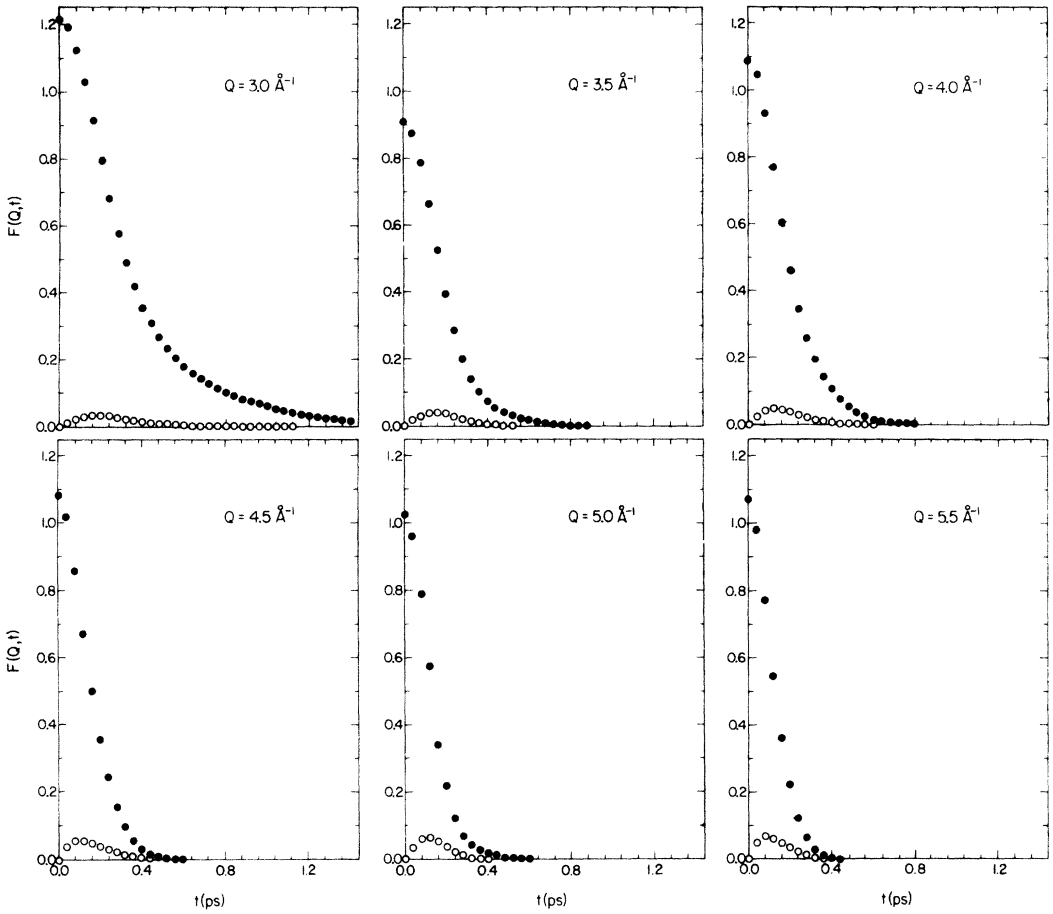

FIG. 10. Intermediate-scattering function $F(Q,t)$ for six values of $Q \geq 3.0$ Å^{-1}. The real and imaginary parts are represented by closed and open circles, respectively.

ple liquid metal over the complete range of interesting wave vectors. As such, the combined results offer the possibility of detailed comparisons with both simple models and molecular-dynamics calculations. In the following paper,[13] the results are compared with molecular-dynamics calculations using the potential of Ref. 6.

It should be noted that for $Q \geq 1.25$ Å^{-1}, there is *no* evidence of peaks at finite ω in $\tilde{S}(Q,\omega)$ at constant Q. Thus, we find no evidence of propagating collective excitations in this range of wave vectors, in contrast to the regime[14] $Q \leq 1.0$ Å^{-1}. We feel that this distinction is a fundamental property of the liquid, and that it is not useful to discuss "dispersion curves" in the regime $Q \geq 1.25$ Å^{-1}. Such curves have been derived by Cocking[8] and by Suck and Gläser[24] by two distinct procedures. The former author used a 2.0-meV incident beam, and identified the peaks in the time-of-flight spectra with a dispersion relation for the liquid. As discussed in Sec. II, the peaks in such data are sim-

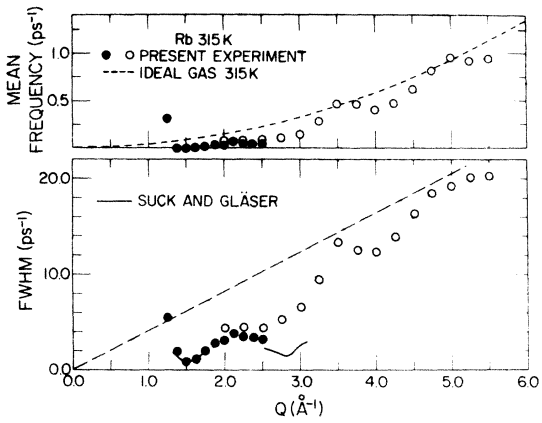

FIG. 11. Position of the peak in $S(Q,\omega)$, and the full width at half-maximum of the peak. The results for the ideal gas, and the measurements of Suck and Gläser (Ref. 24) are also shown. The symbols have the same significance as in Fig. 3.

ply a result of the technique of measurement, and vanish when the data are reduced to $S(Q, \omega)$ at constant Q. In fact, since the time-of-flight data measure a quantity proportional to $E_f^2 S(Q, \omega)$, where E_f is the final energy, the data are closely related to $\omega^2 S(Q, \omega)$ when $E_f \gg E_0$. As is well known, this function always has a peak at finite ω, even for the ideal gas. Suck and Gläser derive their "dispersion curve" by considering the peaks in $S(Q, \omega)$ *at constant* ω. In this case, the peaks are real, but they do not represent propagating collective excitations, since no peaks occur at finite ω values in $S(Q, \omega)$ at constant Q. Such a result could arise from a dispersion curve with infinite slope $(d\omega/dq)$, but as the derived curves have a finite slope, this is not the case here.[29]

The present results indicate definite differences between the scattering functions of liquid Rb and liquid Ar. Nonetheless, the scattering functions are in many respects similar, in contrast to that of a molten salt. Recent coherent neutron scattering experiments on RbBr (Ref. 4) at 973 K show marked differences in $S(Q)$ as well as in $\tilde{S}(Q, \omega)$. These differences no doubt result from the strong Coulomb forces in the ionic liquid.

The present results suffer in the range $2.5 \lesssim Q \lesssim 3.5$ Å^{-1}, because of poor energy resolution in experiment 2. A further experiment, using an incident energy of 20–25 meV, should provide useful information about the detailed behavior of $\tilde{S}(Q, \omega)$ in this interesting range of wave vectors. Such an experiment has been performed by Suck and Gläser,[30] and is presently being analyzed.

Experiments at higher temperatures, both in this range and in the range $Q < 1.0$ Å^{-1}, would help toward a fuller understanding of this material. The latter experiment would be a formidable task, in view of the long counting times required.

It would also be useful to measure the incoherent scattering function of an alkali metal over a wide range of momentum transfers, as was done for argon, in order to compare experiment with models which use the incoherent scattering function as input. One method of attempting this might be to scale the present results for the coherent scattering function of Rb to make them applicable to Na, and to use these results to obtain the incoherent scattering function of sodium from the measured mixture of coherent- and incoherent-scattering functions. The moments of the final result would serve as a useful check of the validity of this approach. Before doing this, detailed molecular dynamics calculations on sodium would be useful in order to evaluate the applicability of this technique.

Note added in proof. We have been informed by Suck (private communication) that the discrepancy between the results of Ref. 24 and the present results for the FWHM near $Q = 2.8$ Å^{-1} was due to difficulties with their correction for empty-container scattering. There is no discrepancy between their reanalyzed measurements and the present results.

ACKNOWLEDGMENTS

The authors thank R. Kleb and G. E. Ostrowski for valuable technical assistance. Useful and provocative discussions with D. L. Price, A. Rahman, K. S. Singwi, and others are gratefully acknowledged. We also thank W. Gläser for communicating some of the results of Suck and Gläser prior to publication.

---

*Based on work performed under the auspices of the U. S. Atomic Energy Commission.

†Present address: Institut Laue-Langevin, BP 156 Centre de tri, 38042 Grenoble, Cédex, France.

[1] J. R. D. Copley, D. L. Price, and J. M. Rowe, Nucl. Instr. Methods 107, 501 (1973). An erratum has been accepted for publication.

[2] J. R. D. Copley, Comp. Phys. Commun. (to be published). Copies of the program are available from the Argonne Code Center, Argonne National Laboratory, Building 221, Argonne, Ill. 60439. See also, F. G. Bischoff, Ph.D. thesis (Rensselaer Polytechnic Institute, 1970) (unpublished); and F. G. Bischoff, M. L. Yeater, and W. E. Moore, Nucl. Sci. Eng. 48, 266 (1972).

[3] K. Sköld, J. M. Rowe, G. Ostrowski, and P. D. Randolph, Phys. Rev. A 6, 1107 (1972).

[4] D. L. Price and J. R. D. Copley (unpublished).

[5] J. R. D. Copley, B. N. Brockhouse, and S. H. Chen, in *Neutron Inelastic Scattering* (IAEA, Vienna, 1968), Vol. I, p. 209; J. R. D. Copley, Ph.D. thesis (McMaster University, Hamilton, Ontario, 1970) (unpublished); J. R. D. Copley and B. N. Brockhouse, Can. J. Phys. 51, 657 (1973).

[6] W. M. Shyu, K. S. Singwi, and M. P. Tosi, Phys. Rev. B 3, 237 (1971). See also, D. L. Price, W. M. Shyu, K. S. Singwi, and M. P. Tosi, Argonne National Laboratory Report No. ANL-7761, 1970 (unpublished). The equilibrium properties of liquid Rb were calculated by D. L. Price (private communication).

[7] J. R. D. Copley, Acta Crystallogr. A 26, 376 (1970); F. F. Y. Wang and D. E. Cox, Acta Crystallogr. A 26, 377 (1970); P. Meriel, C. R. Acad. Sci. (Paris) B 270, 560 (1970).

[8] S. J. Cocking, Adv. Phys. 16, 189 (1967).

[9] *Neutron Cross Sections*, BNL 325, 2nd ed. (U. S. GPO, Washington, D.C., 1958).

[10] A. Rahman, in *Proceedings of the Sixth IUPAP Conference on Statistical Mechanics*, edited by S. A. Rice, K. F. Freed, and J. C. Light (University of Chicago

Press, Chicago, 1972), p. 177. This article contains a review of recent developments in memory-function models for the coherent-scattering function.

[11]J. M. Rowe and K. Sköld, in *Neutron Inelastic Scattering 1972* (IAEA, Vienna, 1972), p. 413. In this article several models are compared directly to the data of Ref. 3. A reasonably comprehensive list of references is included.

[12]B. Jacrot, N. Kroó, and T. Springer, in Ref. 11, p. 859.

[13]A. Rahman, following paper, Phys. Rev. A 9, 1667 (1974).

[14]J. R. D. Copley and J. M. Rowe, Phys. Rev. Lett. 32, 49 (1974).

[15]L. Van Hove, Phys. Rev. 95, 249 (1954).

[16]R. Kleb, G. E. Ostrowski, D. L. Price, and J. M. Rowe, Nucl. Instrum. Meth. 106, 221 (1973).

[17]Since we made these measurements we have established by a simple calculation, for the case of an isotropic scatterer, that absorbing disks (such as were used in the present experiment) serve little purpose unless the separation between disks H is much less than the diameter of the cylinder D. If $H = D$, the multiple scattering is reduced by $\sim 35\%$ from its value in the case where $H \to \infty$.

[18]J. M. Carpenter, Rev. Sci. Instrum. 40, 555 (1969).

[19]K. N. Pathak and K. S. Singwi, Phys. Rev. A 2, 2427 (1970).

[20]D. I. Page, P. A. Egelstaff, J. E. Enderby, and B. R. Wingfield, Phys. Lett. A 29, 296 (1969); B. R. Wingfield, D. I. Page, and J. E. Enderby (private communication).

[21]D. E. Parks, M. S. Nelkin, J. R. Beyster, and N. F. Wikner, *Slow Neutron Scattering and Thermalization* (Benjamin, New York, 1970), p. 54.

[22]Tables of $\tilde{S}(Q,\omega)$ and $F(Q,t)$ may be obtained by writing to Muriel Benz, Solid State Science Division, Argonne National Laboratory, Argonne, Ill. 60439.

[23]See Ref. 11. Note that in an erratum the authors point out an error in their original expression for the Gaussian memory function. The correct expression yields good agreement with experiment.

[24]J.-B. Suck and W. Gläser, in Ref. 11, p. 435.

[25]P. A. Egelstaff, D. I. Page, and C. Duffill, Can. J. Phys. 50, 3062 (1972).

[26]R. A. Cowley and A. D. B. Woods, Can. J. Phys. 49, 177 (1971).

[27]W. J. L. Buyers, V. F. Sears, P. A. Lonngi, and D. A. Lonngi, in Ref. 11, p. 399.

[28]P. G. de Gennes, Physica (Utr.) 25, 825 (1959).

[29]W. Gläser, S. Hagen, U. Löffler, J. B. Suck, and W. Schommers, *The Properties of Liquid Metals, Proceedings of the Second International Conference* (Taylor and Francis, London, 1973). In this paper, the authors examine the coherent neutron scattering from Cu, Ga, and Rb in some detail and state conclusions similar to those presented here. A limited comparison to molecular-dynamics calculations is presented for liquid Rb.

[30]J.-B. Suck and W. Gläser (private communication).